

# MSP2018 Late-Breaking Abstracts

Presenter	Affiliation	Title	ID
Toshiki Sugai	Toho Univ.	Development of Ion Trap Ion Mobility Measurement System and Observation of Observation of Nanomaterials	1P-52 (LB)
Yu-Cen Sun	Acromass	Detection of Intact Biomolecular Ions by inTrap MALDI and Charge-Sensing Particle Detector	1P-53 (LB)
Moe Okuyama	OSAKA UNIV.	Comparison of Metabolites in Saliva and Gingival Crevicular Fluid for Searching Periodontal Disease Biomarkers	1P-54 (LB)
Yoshiteru Iinuma	OIST	Comparison of CO <sub>2</sub> and N <sub>2</sub> drift gas for the separation of isobaric isomer compounds in a travelling wave ion mobility mass spectrometry	2P-63 (LB)
Daisuke Miura	SUNTORY	Development of Sample Preparation Method of Mass Spectrometry Imaging toward Metabolite Localization Analysis with Higher Sensitivity and Reproducibility	2P-64 (LB)
Alejandro Villar-Briones	OIST	LC-MS-Compatible Salt-free High-Resolution Microfractionation of Tryptic Peptides at Nanogram Levels	2P-65 (LB)
Garwin Pichler	PreOmics	Improved iST workflows for the streamlined analysis of tissues and high-throughput preparation of samples using isobaric labeling	3P-51 (LB)
Chia-Li Han	Taipei Medical Univ.	A Oncoproteogenomics Strategy for Multiplexed Screening of EGFR Mutations in Non-small-cell Lung Cancer	3P-52 (LB)
Radoslaw Sobota	A*STAR, Singapore	High Resolution - Mass Spectrometry Cellular Thermal Shift Assay (HR-MS-CETSA)-post-translational modifications impact on thermal protein stability	3P-53 (LB)
Yi Wang	BPRC	Urine proteome profiling predicts lung cancer from control cases and other tumors	3P-54 (LB)
Hee-sub Yun	HEE-SUB YUN	Novel interaction of RSK3 and I $\kappa$ B $\alpha$ induced cell growth and survival in breast cancer cells	3P-55 (LB)
Shujuan Wang	BPRC	Quantitative analysis of ERBB protein complex assembly as a diagnostic tool for abnormal signaling in cancer cells	4P-41 (LB)
Hui Zhou	Jilin University	Urinary metabolomics study of the therapeutic mechanisms of Ding-Zhi-Xiao-Wan against Alzheimer's disease rat model using UPLC-Q-TOF-MS	4P-42 (LB)
Zhixin TIAN	Tongji University	Large-scale Identification and Visualization of N-Glycome with Primary Structures Using GlySeeker	3A-02-P-1555

## 1P-52 (LB)

### Development of Ion Trap Ion Mobility Measurement System and Observation of Observation of Nanomaterials

(Department of Chemistry Toho University)

Y. Hoshino, R. Miyamoto, F. Uchiyama, N. Terada, ○T. Sugai

**Keywords:** Nanomaterials, Mobility, Ion Trap

Ion mobility spectrometry (IMS) has been utilized to reveal novel information on nano materials<sup>1,2</sup>. However, no long-term successive measurement has been performed with IMS usually because of the lack of trap functions, which limits the resolution and the varieties of information. Recently ion trap ion mobility system has been developed to enhance the resolution and long-term evolution of biomolecules. The trap time, however, is restricted to less than 2 seconds and no other measurement such as optical spectroscopy is combined<sup>3</sup>. Here we present long-term successive IMS measurements with optical measurements on nano materials such as graphene quantum dots<sup>4</sup> (GQD) and metal clusters as single molecules.

Fig. 1 shows TEM images of GQD with few layers of graphene sheets and with an average diameter around 20 nm. The sample was measured with our system. Fig. 2 shows the long-term time dependence of the observed velocities of each GQD molecule with various charges. Single GQD molecules can be observed and the structures and charge states are conserved for up to 7 hours. The diameter evaluated to be 20 nm from the velocity and the estimated charge state, which is in good agreement with that from the TEM observation. We have also succeeded to observe noble metal clusters. Optical spectroscopy on each molecule are also in progress by utilizing thus realized long-term trap functions.

#### References

- 1) T. Sugai *et al.*, *J. Am. Chem. Soc.* **123**, 6427- 6428 (2001).
- 2) T. Sugai, *J. Mass. Spectrom. Soc. Jpn.* **58**, 47-73 (2010).
- 3) F. Fernandez-Lima *et al.*, *J. Ion Mobil. Spec.* **14**, 93-98 (2011)
- 4) R. Sekiya *et al.*, *Chem. Eur. J.*, **22**, 8198-8206 (2016).

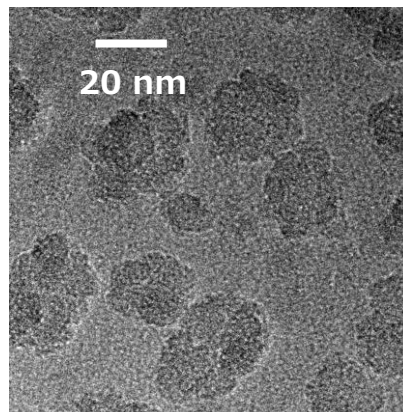


Fig. 1 TEM images of GQD

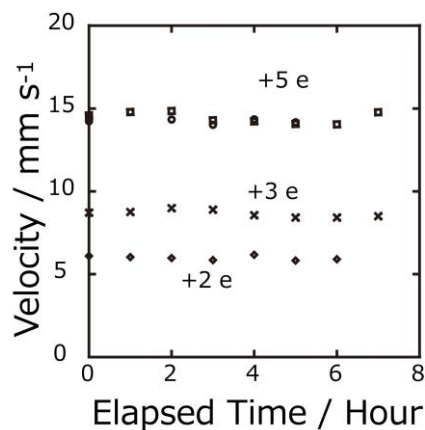


Fig. 2 Observed velocity of GQD with various charges

## 1P-53 (LB)

### inTrap MALDI と電荷センシングでの粒子検出器によって構造完全な生体分子イオンを直接検出する方法

(譜光儀器株式会社<sup>1)</sup>)

スヌーツェン    チョウスーウェイ    リーイクン    ヨンイヤオシン    ヤンシージェ    チョンジュンイェン  
孫宇岑<sup>1</sup>・○周思瑋<sup>1</sup>・李怡坤<sup>1</sup>・曾耀興<sup>1</sup>・楊世韻<sup>1</sup>・鄭俊彦<sup>1</sup>

### Detection of Intact Biomolecular Ions by inTrap MALDI and Charge-Sensing Particle Detector

(AcroMass Technologies, Inc.<sup>1</sup>)

Conan Sun<sup>1</sup>, ○Szu-Wei Chou<sup>1</sup>, Yi-Kun Lee<sup>1</sup>, Yao-Hsin Tseng<sup>1</sup>, Shin-Chien Yang<sup>1</sup>, Chun-Yen Cheng<sup>1</sup>

**Keywords:** charge detection, ion trap mass spectrometry, MALDI, intact protein

We have developed a novel ion cloud detector called charge-sensing particle detector (CSPD, Figure 1), which is used in mass spectrometry to unbind the detectivity limitation of high-mass biomolecular ions, such as intact proteins. Whenever an ion cloud suddenly approaches the Faraday tray on the CSPD, the weak yet-fast charging along with incoming event is nonlinearly converted into to a sharp pulse signal.

The setup of mass spectrometer (Figure 2), includes inTrap MALDI as a highly efficient ion source and a quadrupole ion trap (3D Paul Trap) as a mass-to-charge analyzer. Two phase-synthesized RF waveforms (main & auxiliary) are sent to the trap electrodes for intact-molecular mass spectrum, via ion trapping, adiabatic cooling, phase synchronization and unstable ejection. The ions are directly inTrap prepared, as depicted in Figure 3, with no ion guide for ion transmission.

One example is the mass spectrum of biomolecule Cytochrome C, via unstable ejection and synchronization aid from auxiliary pulses (shown in Figure 4). Beside the primary peak of pure Cyto C<sup>+</sup>, CSPD finesse responses every finely-resolved matrix-modified Cyto C<sup>+</sup> cloud in its tail, and goes without ambiguous overshooting. CSPD is a bipolar device, right for the general case with both positive and negative ions.

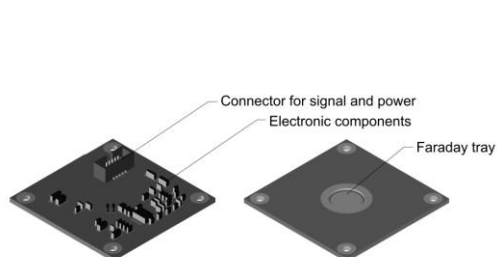


Fig.1. The charge-sensing particle detector

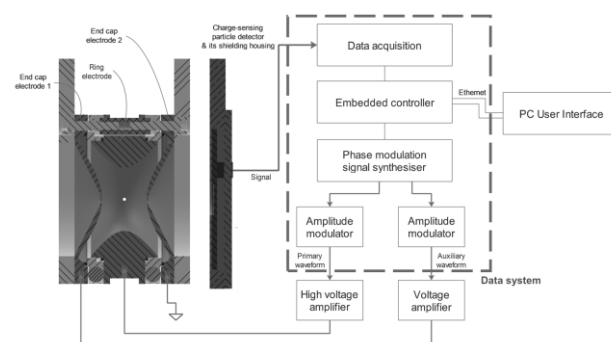


Fig.2. The brief functional chart

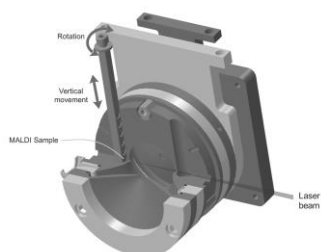


Fig.3. inTrap MALDI

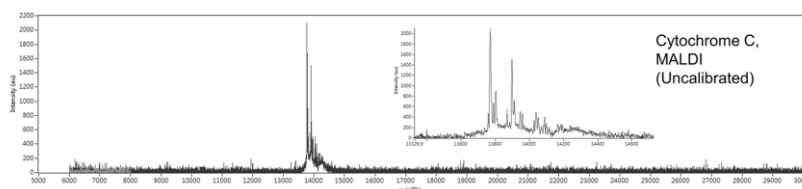


Fig.4. Uncalibrated MALDI ion trap mass spectra of Cytochrome C

### References

- 1) Raymond E. March, Journal of Mass Spectrometry, Vol. 32, 351E369 (1997).
- 2) Urs P. Schlunegger *et al.*, Rapid Commun. Mass Spectrom. 13, 1792–1796 (1999).

# 1P-54 (LB)

## 歯周病バイオマーカー探索に向けた唾液と歯肉溝滲出液内代謝物の比較

(阪大院理)

おくやまもえ おおすがじゅんいち とよだみちと  
○奥山萌恵・大須賀潤一・豊田岐聡

### Comparison of Metabolites in Saliva and Gingival Crevicular Fluid for Searching Periodontal Disease Biomarkers

(Osaka University)

○M. Okuyama, J. Osuga, M. Toyoda

**Short Abstract:** Periodontal disease is one of the most concerned threats to oral health. Therefore, it is desired to establish new method of on-site analysis to diagnose periodontal disease conditions. In the previous research, nineteen metabolites in gingival crevicular fluid (GCF) were identified. Additionally, it was suggested that periodontitis progression could be observed with a changing metabolite profile. In this study, saliva with pretreatment was analyzed using Gas Chromatography/ Mass Spectrometry (GC/MS). As a preliminary result, metabolites in saliva and GCF were compared. It seems that concentrations of metabolites in saliva are lower than those in GCF.

**Keywords:** Periodontal disease, GC/MS

本研究では、歯周病オンサイト診断法開発を目標としたバイオマーカー探索をおこなう。歯周病は歯を支える歯周組織が細菌に侵され破壊される感染症であり、進行に伴って歯周組織の破壊が高度化することから、成人が歯を喪失する第一位の原因である。また、糖尿病や心臓病などの全身疾患との相互関連性も近年報告されている。しかしその病態の的確な評価法はなく、歯周病の進行度合いも個人差があるため、オンサイトで迅速かつ簡便に評価ができる新規診断法の確立が望まれている。先行研究において、歯周ポケットから採取可能な歯肉溝滲出液を用いたバイオマーカー探索が行われ、進行度合いに応じて有意差が見られるバイオマーカー候補化合物が19種類特定された<sup>1</sup>。歯肉溝滲出液は患部から直接採取できるが、一方で採取は歯科医しか行えない。そこで、非侵襲的で場所を選ばず容易に採取可能な唾液による診断法の開発を行えないか考えた。ここでは歯周病診断の試料に唾液を用いるための基礎的な検討として、唾液と歯肉溝滲出液を分析し検出される代謝物がどの程度共通しているか調べた。

前処理として、参考文献2にならって実試料から親水性化合物を抽出、濃縮、乾燥させ、誘導体化した。その後、GC/MS法で一斉分析をおこなった。内部標準試料として2-イソプロピルリンゴ酸を用い、相対面積値による半定量解析をおこなった。

健常者1名の唾液3.0μLと歯肉溝滲出液0.20μLを分析した。計94成分が検出されたうち、両試料から59成分、歯肉溝滲出液のみから16成分、唾液のみから19成分の代謝物が検出された。この結果から、62.8%は唾液と歯肉溝滲出液双方で検出されていることがわかる。しかしながら、検出された化合物のうち、バイオマーカー候補として挙げられている成分に注目すると、13成分が歯肉溝滲出液試料で検出されており、標準品を用いて保持時間とスペクトルを確認した。これらの化合物について、各化合物のベースピークと各化合物と内標との相対面積値をまとめたものをTable.1に示す。ただし、比較のため分析試料の同体積あたりの相対面積値とした。この結果から、両試料で検出された化合物はいずれも唾液試料の方が低い値を示しており、バイオマーカー候補化合物の唾液内代謝物濃度は歯肉溝滲出液と比べて12倍から600倍程度低いことがわかった。本発表では、唾液のサンプル量を増やした時の検出ピーク数や分析法の堅牢性についても議論したい。

<i>m/z</i>	Name	GCF	Saliva
174	Propylamine	1.2E-01	5.5E-03
179	Benzoic acid	8.5E-01	6.9E-03
174	Glycine	4.2E-01	1.0E-02
174	5-Aminovaleric acid	1.7E-01	8.3E-03
217	Ribose	6.0E-02	9.7E-05
174	Putrescine	2.0E-01	3.1E-03
217	Myo-Inositol	1.5E-02	3.1E-04
147	Malic acid	5.6E-02	1.4E-03
341	Stearic acid	1.4E+00	1.1E-01
116	L-Alanine	5.6E-02	-
246	L-Glutamic acid	8.9E-01	-
319	D-Galactose	7.4E-02	-
317	L-Lysine	7.6E-03	-

Table.1 Relative intensity of identified metabolites

#### 参考文献

- 1) M. Ozeki et al., Mass Spectrometry 5 : A0047(2016)
- 2) S. Nishiumi et al., Metabolomics 6 : 518-528 (2010)

## 2P-63 (LB)

### Comparison of CO<sub>2</sub> and N<sub>2</sub> drift gas for the separation of isobaric isomer compounds in a travelling wave ion mobility mass spectrometry

(Okinawa Institute of Science and Technology<sup>1</sup>, National Institute for Environmental Studies<sup>2</sup>, Tianjin University Japanese Mass Spectrometry Co.<sup>3</sup>)

○Y. Iinuma<sup>1</sup>, E. Hayakawa<sup>1</sup>, S. Inomata<sup>2</sup>, K. Sato<sup>2</sup>, H. Ren<sup>3</sup>, S. Yue<sup>3</sup>, P. Fu<sup>3</sup>

**Keywords:** Ion Mobility, Travelling Wave Ion Mobility, Environmental Samples, Aerosol, PM

Isobaric isomer compounds are ubiquitous occurrence in ambient atmospheric aerosols. They originate from oxidation processes of anthropogenic and biogenic volatile organic compounds (VOCs) such as aromatic compounds and monoterpenes. For example, monoterpenes are known to produce a series of isobaric isomer compounds such as C<sub>9</sub>H<sub>14</sub>O<sub>4</sub>, C<sub>8</sub>H<sub>12</sub>O<sub>4</sub>, C<sub>10</sub>H<sub>18</sub>O<sub>5</sub>S, and C<sub>10</sub>H<sub>17</sub>NO<sub>7</sub>S. Among these isobaric isomer compounds, C<sub>10</sub>H<sub>17</sub>NO<sub>7</sub>S compounds are still not conclusively structurally characterized to date owing to the lack of knowledge about their formation mechanisms and the difficulty associating with the synthesis of authentic standard compounds<sup>1</sup>). An ion mobility mass spectrometry (IMS-MS) is useful for the structural analysis of such isobaric isomer compounds, as their structural differences lead to their separation in IMS-MS and their mobility data can be used to construct potential structures for a mobility modelling study<sup>2</sup>).

In this study we compare the effects of drift gas types on the separation of C<sub>10</sub>H<sub>17</sub>NO<sub>7</sub>S compounds in a travelling wave ion mobility mass spectrometer (Waters SYNAPT G2-S). These isomeric compounds produce very similar fragment ions that are difficult to associate with the positions of functional groups. A particular focus here is to use CO<sub>2</sub> gas to separate isobaric MS<sup>2</sup> fragment ions that are not well separated with N<sub>2</sub> drift gas, and infer the structures of C<sub>10</sub>H<sub>17</sub>NO<sub>7</sub>S compounds. One of PM<sub>2.5</sub> samples collected in Chengdu, China in June 2016 was selected for the detail investigation.

A commercially available travelling wave ion mobility MS system using the N<sub>2</sub> drift gas tends to work well for the separation of larger ions such as proteins. However, the separation of smaller molecules is challenging as the resolving power is low in comparison to their differences in collisional cross section values (CCS). Figure 1 shows an example of drift-time plots using CO<sub>2</sub> and N<sub>2</sub> for the m/z 247 (C<sub>10</sub>H<sub>15</sub>O<sub>5</sub>S<sup>-</sup>, [M-H]<sup>-</sup>) MS<sup>2</sup> fragment of C<sub>10</sub>H<sub>17</sub>NO<sub>7</sub>S compounds. As can be seen the CO<sub>2</sub> drift gas showed a much better separation for the m/z 247 MS<sup>2</sup> fragments compared to N<sub>2</sub> drift gas, especially for the peaks eluting between 8.5 and 9 minutes. Although this information alone does not lead to the conclusive structural elucidation of the precursor or fragment ions, this data can be useful in the elucidation of the substructures of C<sub>10</sub>H<sub>17</sub>NO<sub>7</sub>S compounds. In this case, the peak detected at 9 min has a longer drifting time than the peak at 9 min, suggesting that either the sulfate group is attached at the terminal position or it has a larger monoterpene skeleton. The result here demonstrates that the separation power of a commercially available travelling wave ion mobility instrument can be improved for small ions with similar CCS when we use a more polarizable drift gas such as CO<sub>2</sub>, and provide more structural information than the N<sub>2</sub> drift gas.

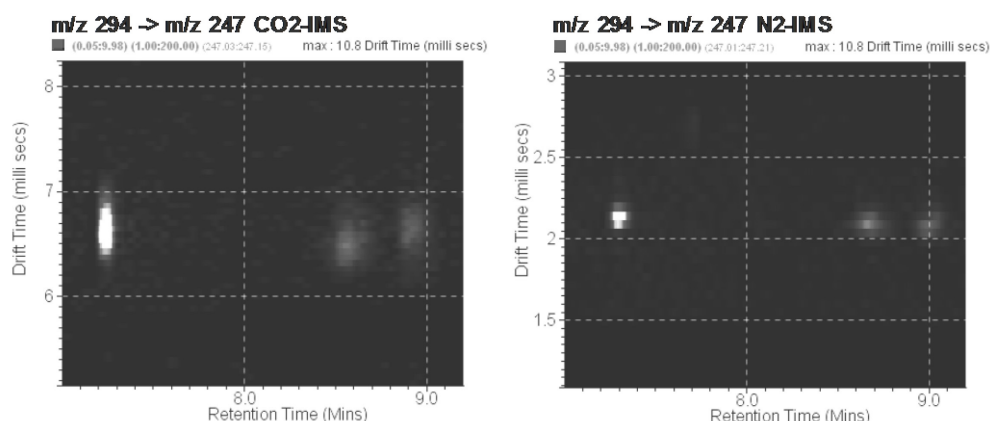


Fig. 1. Drift time as a function of chromatographic retention time using CO<sub>2</sub> (left) and N<sub>2</sub> (right) for the m/z 247 MS<sup>2</sup> fragment [M-H]<sup>-</sup>.

#### References

- 1) B Noziere *et al.*, Chem. Rev., **115**(10), 3919-3983, doi:10.1021/cr5003485 (2015).
- 2) M F Mesleh, *et al.*, J Phys Chem, **100**(40), 16082-16086 (1996).

## 2P-64 (LB)

### 高感度かつ再現性の高い代謝物局在解析をめざした質量分析イメージングの試料調製法の開発

(九大農学研究院<sup>1</sup>・島津製作所<sup>2</sup>)  
いちのせともみ<sup>1</sup>・ふじむらよしのり<sup>1</sup>・やまざきゆうぞう<sup>2</sup>・みうらだいすけ<sup>1</sup>  
一瀬智美<sup>1</sup>・○藤村由紀<sup>1</sup>・山崎雄三<sup>2</sup>・三浦大典<sup>1</sup>

### Development of Sample Preparation Method of Mass Spectrometry Imaging toward Metabolite Localization Analysis with Higher Sensitivity and Reproducibility

(Fac.Agric., Kyushu University<sup>1</sup> & Shimadzu Co.<sup>2</sup>)  
T.Ichinose<sup>1</sup>, ○Y.Fujimura<sup>1</sup>, Y.Yamazaki<sup>2</sup>, D.Miura<sup>1</sup>

**Keywords:** MALDI-MS, Metabolite imaging, Matrix Application, Sublimation, Sensitivity

**Introduction:** Matrix-assisted laser desorption/ionization (MALDI)-mass spectrometry imaging (MSI) is a powerful technique to visualize the distributions of biomolecules without any labeling. In MALDI-MSI experiments, the choice of matrix deposition method is important for acquiring favorable MSI data with high sensitivity and high spatial resolution. Generally, manual or automated spray-coating and automated sublimation methods are recognized as established matrix coating techniques for MSI. Manual or automated spray-coating methods are relatively convenient, but they show low reproducibility of metabolite detection. The automated sublimation is useful to obtain high spatial resolution and high reproducibility, but its signal intensity is often less than the spray-coating method capable of sensitive detection of such metabolites due to a solvent extraction effect. A recrystallization of sublimated matrix in an organic solvent atmosphere is alternative method to the spray-coating method, and effective to improve sensitivity by solvent extraction effect. To date, there have been no other reports of 9-aminoacridine (9-AA)-based sublimation combined with recrystallization, whereas the matrix is useful to ionize endogenous metabolites. Herein, we present a novel matrix deposition method of sublimation coupled with recrystallization using 9-AA.

**Methods/Results:** We attempted to improve the matrix sublimation method by coupling it with a recrystallization reaction with solvent treatment, using 9-AA as a matrix for visualizing the distributions of endogenous metabolites. The matrix vapor deposition system iMLayer (Shimadzu), which can automatically monitor the temperature and thickness of a matrix deposited during sublimation, was used. Our procedure for matrix sublimation and recrystallization on a tissue sample (mouse brain: C57BL/6J, 6 weeks, male) consisted of two steps. The first step was formation of the matrix layer on mouse brain sections by sublimation using iMLayer. The next step was co-crystallization of the matrix and analyte on the tissue, with exposure to solvent vapor to promote recrystallization of the matrix, using a hand-made reaction chamber. We evaluated our proposed procedure for its ability to provide MSI data with high sensitivity, good spatial resolution, and excellent reproducibility, using a MALDI-TOF-MS instrument (AXIMA Performance, Shimadzu). Both a solvent concentration and reaction temperature were optimized to perform a recrystallization of sublimated 9-AA. This optimized method showed excellent reproducibility and spatial resolution compared to the spray-coating method. Furthermore, the recrystallization step after sublimation remarkably improved the detectability of metabolites, including amino acids, nucleotide derivatives, and lipids, compared with the conventional sublimation method. The present method provides an easy, sensitive, and reproducible matrix deposition method for MALDI-MSI of endogenous metabolites.

**Conclusion/Future aspects:** We established a 9-AA sublimation method with coupling to a recrystallization step, which was optimized for the solvent concentration and reaction temperature. This methodology is very simple but provides excellent detection sensitivity for endogenous metabolites and yields highly reproducible data. The present sample preparation method and its optimization strategy could be applied to tissue sections from different types of organisms and other matrices. This method could be used to obtain precise information about the distributions of endogenous molecules, which could be applied to biological discovery and biomarker development.

#### References

- 1) D. Miura *et al.*, *Biochem. Biophys. Res. Commun.*, **496**, 140-146 (2018).
- 2) D. Miura *et al.*, *Anal. Bioanal. Chem.*, **409**, 1697-1706 (2017).

## 2P-65 (LB)

### LC-MS-Compatible Salt-free High-Resolution Microfractionation of Tryptic Peptides at Nanogram Levels

(Okinawa Institute of Science and Technology<sup>1</sup>)

A.Villar-Briones<sup>1</sup>

**Keywords:** sample preparation, proteomics, salt-free, microfractionation, peptides

The intrinsic complexity of enzymatically digested samples is greatly reduced by employing off-line fractionation. The use of C<sub>18</sub> columns with high-pH solvents addresses the problem of buffers that are incompatible with mass spectrometry (MS) and provides a semi-orthogonal separation of the sample compared to traditional low-pH separation with the same column. However, this technique still relies on the use of an ammonium salt as a buffer to achieve the desired chromatographic resolution. Electrostatic Repulsion-Hydrophilic Interaction Chromatography (ERLIC)<sup>1)</sup> presents an attractive solution to this problem by using a salt-free solvent, fully compatible with tandem MS analysis. This technique has most often been implemented using a Weak Anion Exchange (WAX) column with a 4.6-mm i.d., requiring hundred(s) of micrograms of sample. In addition, it uses solvents supplemented with up to 2% formic acid (FA) for elution, which adversely affects ionization efficiency.

**Here we present an optimized method for microfractionation of tryptic digests using ERLIC separation, compatible with sample loads ranging from micrograms to nanograms, using alkaline solvents similar to those for reverse phase separations in tandem with MS.**

To this end, we used a capillary-size WAX column (1-mm i.d.), at a flow rate of 40 µL/min, with water/acetonitrile containing 0.1% FA and 0.05% ammonium hydroxide, delivered by a binary HPLC pump. Sample elution was monitored at 214 nm and fractions were collected in 96-well plates using an autosampler with a MALDI-Spot accessory. Peptide resolution and recovery were evaluated using 10 µg of a tryptic digest of proteins extracted from mouse brain, separated on a 60-min gradient. Fraction volume was ~120 µL. This system achieved a 2x increase in the number of proteins identified, compared to traditional shotgun analysis using the same amount of sample. More low-concentration proteins were revealed due to the reduced complexity of the fractionated sample. Peptide elution profiles were highly reproducible, making this technique suitable for targeted proteomics. In addition, salts from the digestion buffer elute in the chromatographic void volume; hence, they do not influence mass spectrometry.

This method allows us routinely to microfractionate peptides from small biological samples (several micrograms), considerably increasing the number and coverage of identified proteins, with special emphasis on low-abundance components. Separation of peptides in a reduced volume improves their re-suspension prior to LC-MS injection. Although the method presented here was employed off-line, it can easily be adapted for on-line separation (2D LC) with tandem MS, reducing sample handling and machine time.

This optimized method facilitates peptide fractionation using sample amounts similar to those of traditional shotgun proteomics. Therefore, it is especially useful in cases in which other methods cannot be employed due to limited sample and risk of sample loss due to sample dilution or downstream desalting.

#### References

1) Hao P. *et al.*, J Proteome Res. 2010 Jul 2;9(7):3520-6.

## 3P-51 (LB)

### Improved iST workflows for the streamlined analysis of tissues and high-throughput preparation of samples using isobaric labeling

Garwin Pichler<sup>1</sup>; Fabian Hosp<sup>1</sup>; Nils Kulak<sup>1</sup>  
<sup>1</sup>PreOmics GmbH, Planegg/Martinsried, Germany

#### Introduction

Recently, the straightforward and robust in-StageTip (iST) method for streamlined sample processing of various sample types including cell lines and body fluids (e.g. plasma, serum, CSF, urine) was described (Kulak et al., Nat Meth, 2014). Here, we present further developments based on the iST technology.

#### Methods

The iST method is a 3-step procedure performed in a single, enclosed volume, which thereby circumvents the likelihood of contamination and sample loss. Moreover, it allows rapid sample preparation from lysing the sample to ready-to-measure peptides in less than 3 hours while keeping excellent reproducibility and sensitivity. Due to its straightforward nature, the method can readily be performed in a 96-well format on liquid handling robotic systems. The iST workflow is highly compatible with established and novel StageTip based pre-fractionation methods and thereby allows in-depth analysis of complex proteomic samples.

#### Preliminary Data

First, we present the iST-NHS adaptation that allows chemical labeling of peptides in the very same reaction device used for cell lysis, protein denaturation, reduction, alkylation and digestion, thus minimizing sample loss, overall hands-on time and the amount of required chemical labels. Using yeast cells, we employed this iST-NHS approach and compared different ratios of tandem mass tag (TMT) reagents per  $\mu\text{g}$  of peptides input material. While most labeling workflows utilize a TMT to peptide ratio of 8:1, we found that a ratio of 4:1 results in the highest number of identified peptides while still achieving labeling efficiencies of more than 99.5% using the iST-NHS method. In addition, the iST-NHS method is fully compatible with 96well plate formats and automated robotic systems enabling high-throughput isobaric labeling experiments.

Second, we present an improved iST workflow for the lysis of tissue (fresh brain, heart and liver samples, as well as FFPE samples) directly in the reaction device used for the downstream sample preparation, thus avoiding lysate transferring steps and minimizing sample loss. We present identification of 6,000-10,000 proteins for the aforementioned tissue types demonstrating in-depth proteome analysis with minimal sample preparation efforts. With this improved iST workflow, up to 24 tissue samples can be prepared in parallel and in less than 3 hours from wet tissue to ready-to-measure peptides.

#### Novel Aspect

The new iST developments enable streamlined analysis of tissues and high-throughput preparation of chemically labeled samples.

## 3P-52 (LB)

### A Oncoproteogenomics Strategy for Multiplexed Screening of EGFR Mutations in Non-small-cell Lung Cancer

Chi-Ting Lai<sup>1,2</sup>, Wai-Kok Choong<sup>3</sup>, Yi-Ju Chen<sup>1</sup>, Hui-Yin Chang<sup>3</sup>, Ting-Yi Sung<sup>3</sup>, Hsuan-Yu Chen<sup>2,4</sup>, Yu-Ju Chen<sup>1,2\*</sup>, Chia-Li Han<sup>5\*</sup>

<sup>1</sup>*Institute of Chemistry, Academia Sinica, Taipei, Taiwan;* <sup>2</sup>*Genome and Systems Biology Degree Program, National Taiwan University, Taipei, Taiwan;* <sup>3</sup>*Institute of Information Science, Academia Sinica, Taipei, Taiwan;* <sup>4</sup>*Institute of Statistical Science, Academia Sinica, Taipei, Taiwan;* <sup>5</sup>*Master Program in Clinical Pharmacogenomics and Pharmacoproteomics, College of Pharmacy, Taipei Medical University, Taipei, Taiwan*

Oncogenes with somatic mutations contribute to the development and progression of cancers. However, the expression levels of mutation bearing oncogenes and their translated protein variants are largely unexplored. Thus, we aimed to develop a mass spectrometry (MS)-based oncoproteogenomics strategy for multiplexed screening of tumor-specific mutations on oncoproteins. The non-small-cell lung cancer (NSCLC) which harbor different *EGFR* genotypes were used as study model. The oncoproteogenomics strategy integrated bioinformatics analysis of mutant protein sequences for protease prediction, affinity purification of EGFR protein complex, parallel enzymatic gel-assisted digestions, LC-MS/MS analysis, and customized database searching using multiple engines, for unambiguous identification of 34 mutated and 33 wild-type EGFR proteins. The abundances of cellular wild-type and mutant EGFR proteins were measured using LC-PRM-MS in a series of NSCLC cell lines. The results revealed concomitant and heterogeneous expressions of mutant and wild-type EGFR proteins in NSCLC. We expected that our developed oncoproteogenomics strategy can precisely determine the multiple somatic mutations at protein level and provide a better understanding towards the molecular impact of *EGFR* genetic mutations during tumor progression and adaption to tyrosine kinase inhibitor treatments.

#### Keywords

EGFR, lung cancer, oncoproteogenomics

## 3P-53 (LB)

### High Resolution - Mass Spectrometry Cellular Thermal Shift Assay (HR-MS-CETSA)-post-translational modifications impact on thermal protein stability

School of Biological Sciences, Nanyang Technological University, Singapore<sup>1</sup>. Institute of Molecular and Cell Biology (IMCB), Agency for Science, Technology and Research (A-STAR), Singapore<sup>2</sup>, Department of Oncology-Pathology, Karolinska Institutet, Stockholm, Sweden<sup>3</sup>

Lingyun Dai<sup>1</sup>, Tianyun Zhao<sup>1</sup>, Liyan Chen<sup>1</sup>, Chris Soon Heng Tan<sup>2</sup>, Yan Ting Lim<sup>1</sup>, Par Nordlund<sup>1,2,3</sup>,

○Radoslaw M. Sobota<sup>2</sup>

**Keywords:** PTM, Thermal Shift Assay, MS-CETSA, drug target deconvolution

Observation of the proteins thermal stability towards increasing temperature forms the foundation for methods that explore thermally induced protein unfolding. Heat treatment induced protein unfolding and aggregation can be graphically presented as a sigmoidal melting curve. It was shown that ligand engagement changes the functional state of the protein and induces thermal shift. MS- based Cellular Thermal Shift Assay (CETSA) monitors thermal induced unfolding of individual proteins in lysates/intact cells/tissue samples using quantitative mass spectrometry. To further extend CETSA application, here we proposed high resolution MS-CETSA to increase a target specificity. We investigated further impact of post-translational modifications on the protein stability. We were able to detect in the sample with limited input more than 5000 distinct phosphorylation residues, representing over 5000 unique melting profiles. We demonstrated that phosphorylated proteins exhibit different stability towards increasing temperature. Results point destabilizing effect of the phosphorylation, although detailed mechanism has to be further determined. Furthermore, presented method could help to identify functional phosphorylation sites in the protein which occupancy would be reflected in protein stability. The Cellular PTM resolved MS-CETSA has potential to add a valuable dimension to pre-clinical drug development defining drug target engagement and off-target effects in relevant tissue systems.

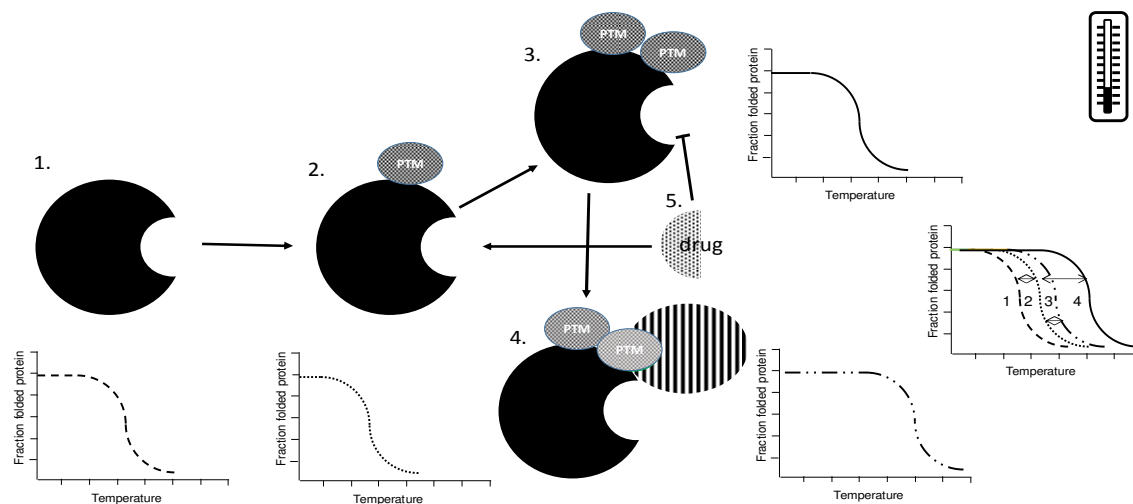


Figure1. Influence of PTM on protein stability - High resolution PTM resolved MS-CETSA principle. (1) Baseline- unmodified protein with distinct melting properties. (2). Modified protein with PTM affecting melting behaviour. Additional PTM could affect melting properties directly (3) or indirectly (4) by triggering new complex formation or cellular localization context. (5) Drug candidate distinguishing specific PTM state and preventing protein further activity.

1. Thermal proximity coaggregation for system - wide profiling of protein complex dynamics in cells. Tan Soon Heng Ch. Go Ka Diam, Bisteau X., Dai Lingyun, Prabhu N., Ozturk B., Lim YT., Sreekumar L., Chern Han Yong, Lengqvist J., Tergaonkar V., Kaldis P., **Sobota R.M.**, Nordlund P. *Science* 08 Feb 2018: eaan0346 DOI: 10.1126/science.aan0346
2. Dual Blockade of the Lipid Kinase PI5P4Ks and Mitotic Pathways Leads to Cancer-selective Lethality Kitagawa, M., Liao, Pei-Ju, Wong J., Cheng Shang See, Minami, N., Sampetean, O., Saya, H., Dai Lingyun, Prabhu, N., Go Ka Diam, **Sobota, R.**, Larsson, A., Nordlund P., McCormick, F., Ghosh S., Epstein, D., Dymock, B., Sang Hyun Lee. *Nature Communications*, 2017 Dec 19;8(1):2200. doi: 10.1038/s41467-017-02287-5

## 3P-54 (LB)

### Urine proteome profiling predicts lung cancer from control cases and other tumors

Chunchao Zhang<sup>3</sup>, Wenchuan Leng<sup>1,2</sup>, Changqing Sun<sup>2</sup>, Tianyuan Lu<sup>1</sup>, Zhengang Chen<sup>2</sup>, Xuebo Men<sup>2</sup>, Yi Wang<sup>1,3</sup>, Guangshun Wang<sup>2</sup>, Bei Zhen<sup>1,2</sup>, Jun Qin<sup>1,2,3</sup>

1. State Key Laboratory of Proteomics, National Center for Protein Sciences (The PHOENIX Center, Beijing), Beijing Proteome Research Center, Beijing, 102206, China
2. Joint Center for Translational Medicine, Tianjin Baodi Hospital, Tianjin, 301800, China
3. Alkek Center for Molecular Discovery, Verna and Marrs McLean Department of Biochemistry and Molecular Biology, Department of Molecular and Cellular Biology, Baylor College of Medicine, Houston, Texas 77030, USA

Development of noninvasive, reliable biomarkers for lung cancer diagnosis has many clinical benefits knowing that most of lung cancer patients are diagnosed at the late stage. For this purpose, we conducted proteomic analyses of 231 human urine samples in healthy individuals (n = 33), benign pulmonary diseases (n = 40), lung cancer (n = 33), bladder cancer (n = 17), cervical cancer (n = 25), colorectal cancer (n = 22), esophageal cancer (n = 14), and gastric cancer (n = 47) patients collected from multiple medical centers. By random forest modeling, we nominated a list of urine proteins that could separate lung cancers from other cases. With a feature selection algorithm, we selected a panel of five urinary biomarkers (FTL: Ferritin light chain; MAPK1IP1L: Mitogen-Activated Protein Kinase 1 Interacting Protein 1 Like; FGB: Fibrinogen Beta Chain; RAB33B: RAB33B, Member RAS Oncogene Family; RAB15: RAB15, Member RAS Oncogene Family) and established a combinatorial model that can correctly classify the majority of lung cancer cases both in the training set (n = 46) and the test sets (n = 14 – 47 per set) with an AUC ranging from 0.8747 to 0.9853. A combination of five urinary biomarkers not only discriminates lung cancer patients from control groups but also differentiates lung cancer from other common tumors. The biomarker panel and the predictive model may be used as an auxiliary diagnostic tool along with imaging technology for lung cancer detection.

## 3P-55 (LB)

### Novel interaction of RSK3 and I $\kappa$ B $\alpha$ induced cell growth and survival in breast cancer cells

Hee-Sub Yun<sup>1,3</sup>, Sung Ho Yun<sup>1</sup>, Eun-Hee Han<sup>1,2</sup>, Sung hoon Choi<sup>1</sup>, Ju hee Park<sup>4</sup> Young-Ho Chung<sup>1,4</sup>

<sup>1</sup>Division of Bioconvergence Analysis, Drug & Disease Target Group, Korea Basic Science Institute(KBSI), Ochang, Republic of Korea; <sup>2</sup>Department of Functional Genomics, University of Science and Technology (UST), Daejeon, Republic of Korea; <sup>3</sup>Korea University, Seoul, Republic of Korea; <sup>4</sup>GRAST, Chungnam National University, Daejeon, Republic of Korea

**Keywords:** Protein-Protein Interaction (PPI), Breast Cancer cells, RSK3, I $\kappa$ B $\alpha$ , Inhibitor

A number of cancer-related biological processes are mediated by protein-protein interaction (PPIs). Therefore, targeting PPIs are emerging as a promising new class of drug targets. But, although PPIs have essential role in cancer diseases, there are few PPIs target as a therapeutic targets in breast cancer. The RSK (90 kDa ribosomal S6 kinase) family comprises a group of highly related serine/threonine kinases that regulate diverse cellular processes, including cell survival, proliferation, growth. Although RSK3 was initially suggested to play positive roles in cell proliferation, a detailed functions and mechanisms are currently unknown. Our group has over the 500 fluorescence tagging kinase vector libraries for screen of kinase PPI as a drug target. Several candidates have been identified as RSK3 binding partner through CUPID analysis. I $\kappa$ B $\alpha$  is one of the RSK3 novel binding partner and is phosphorylated by active RSK3. Besides, A screened PPI inhibitor targeting RSK3/I $\kappa$ B $\alpha$  complex which is playing anti-cancer activity in breast cancer cells such as cell proliferation and survival. Taken together, these observations suggest that RSK3 phosphorylation and RSK3/I $\kappa$ B $\alpha$  complex formation are may be functionally important in breast tumorigenesis. Indeed, the validation of RSK3/I $\kappa$ B $\alpha$  specific inhibitor can provides a lead to development new anti-cancer drugs.

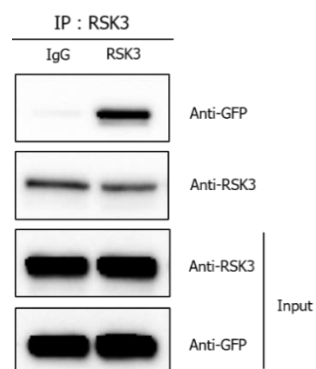


Fig. 1. RSK3/I $\kappa$ B $\alpha$  Direct Interaction (myc/His-RSK3 and GFP-I $\kappa$ B $\alpha$  co-transfected)

### References

- 1) SERRA, Violeta, et al. RSK3/4 mediate resistance to PI3K pathway inhibitors in breast cancer. *The Journal of clinical investigation*, 2013, 123.6: 2551-2563.
- 2) EISINGER-MATHASON, TS Karin; ANDRADE, Josefa; LANNIGAN, Deborah A. RSK in tumorigenesis: connections to steroid signaling. *Steroids*, 2010, 75.3: 191-202.

## 4P-41 (LB)

### Quantitative analysis of ERBB protein complex assembly as a diagnostic tool for abnormal signaling in cancer cells

(State Key Laboratory of Proteomics, Beijing Proteome Research Center, National Center for Protein Sciences (Beijing), Beijing Institute of Lifeomics, Beijing, China<sup>1</sup>, Lunenfeld Tanenbaum Research Institute, Mount Sinai Hospital, Toronto, Canada<sup>2</sup>, Novartis Institutes for Biomedical Research, Cambridge, USA<sup>3</sup>, McGill University Health Centre, Montreal, Canada<sup>4</sup>, Department of Molecular Genetics, University of Toronto, Toronto, Canada<sup>5</sup>)

Shujuan Wang<sup>1#</sup>, Cunjie Zhang<sup>2#</sup>, Adrian Pasculescu<sup>2</sup>, Pan Zhang<sup>1</sup>, Sihui Li<sup>1</sup>, Xiaojing Wu<sup>1</sup>, Xiao Li<sup>3</sup>, Rita Das<sup>3</sup>, Qing Sheng<sup>3</sup>, Lorne Taylor<sup>2,4</sup>, Vivian Nguyen<sup>1</sup>, Tony Pawson<sup>2,5</sup>, Carl Uli Bialucha<sup>3</sup>, Karen Colwill<sup>2\*</sup>, Yong Zheng<sup>1\*</sup>

#: equal contribution

**Keywords:** quantitative mass spectrometry, protein complex, drug resistance

Proteins rarely act by their own but rather as part of large protein complexes formed through dynamic non-covalent protein-protein interactions in response to specific environmental cues. Precisely controlled assembly of protein complexes is critical for the fidelity and magnitude of downstream signaling transduction while its dysregulation leads to aberrant signaling and cancer. Identifying abnormal protein complex formation is key to understand underlying mechanisms of oncogenesis.

We developed an affinity purification and quantitative mass spectrometry-based workflow (AP-MRM and AP-PRM) to quantify 37 interacting proteins in ERBB-mediated protein complexes in 19 cancer cell lines both in basal and ligand stimulated states. ERBB family members are “driver genes” in several cancers including breast cancer. We show that the intrinsic differences between cell lines is the biggest differential as the cell lines varied significantly in the type and number of proteins recruited to the complex. Temporal analysis of ERBB complexes in three breast cancer cell lines suggested that ERBB complexes tend to assembled in a functionally distinct modular fashion in individual cell line which may correlate with prejudicial activation of downstream signaling. Thus, the quantitative characteristics of key protein complexes may serve as a diagnostic tool to identify rewired signaling in cancer.

## 4P-42 (LB)

### Urinary metabolomics study of the therapeutic mechanisms of Ding-Zhi-Xiao-Wan against Alzheimer's disease rat model using UPLC-Q-TOF-MS

(Department of Chemistry and Pharmacy, Zhuhai College of Jilin University, Zhuhai 519041, China<sup>1</sup>  
National Center for Mass Spectrometry in Changchun, Changchun Institute of Applied Chemistry, Chinese Academy of Sciences, Changchun 130022, China<sup>2</sup>)

Yimin Wang<sup>1</sup>, ○Hui Zhou<sup>1</sup>, Shu Liu<sup>2</sup>, Zifeng Pi<sup>2</sup>, Yufei Sun<sup>2</sup>, Zhiqiang Liu<sup>2</sup>

**Keywords:** Metabolomics, Ding-Zhi-Xiao-Wan, Alzheimer's disease

**Background:** As a well-known traditional Chinese medicine (TCM) formula, Ding-Zhi-Xiao-Wan (DZXW) is commonly used for the treatment of mental disorders, especially amnesia and depression<sup>1</sup>. The aim of this study was to investigate the potential curative mechanisms of DZXW on learning and memory in A $\beta$ <sub>25-35</sub> peptide-induced Alzheimer's disease (AD) rat model.

**Methods:** Rats were injected with A $\beta$ <sub>25-35</sub> peptide in bilateral hippocampus CA1 area<sup>2</sup>. After injection 7 days, DZXW were administered once daily for 30 days. Learning and memory abilities tests were then performed by Morris water maze. Furthermore, a urinary metabolomics study was carried out based on ultra high-performance liquid chromatography coupled with quadrupole time-of-flight mass spectrometry (UPLC-Q-TOF-MS), and followed with multivariate analysis to screen potential biomarkers.

**Results:** DZXW administration significantly improved dysmnnesia in Morris water maze ( $P < 0.05$ ) compared to the model group. A total of 28 metabolites were identified as potential biomarkers of AD. The main metabolism pathway in which DZXW affected on AD rats were taurine and hypotaurine metabolism, citrate cycle metabolism, purine metabolism, vitamin B6 metabolism and so on. These findings begin to illuminate therapeutic mechanisms of DZXW upon anti-oxidant protection, energy metabolism regulation, neurons protection and intestinal microbes improvement against AD.

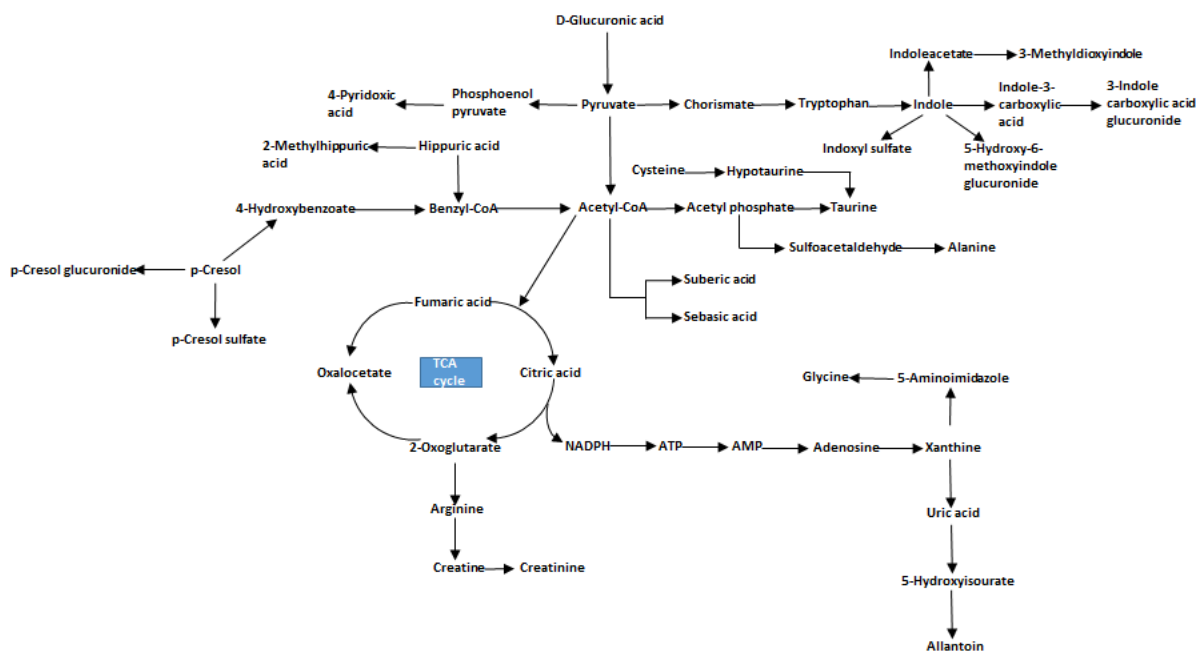


Fig.1. Correlation networks of main potential biomarkers in response to the therapeutic effects of DZXW on AD rats

#### References

- 1) Lu Xu *et al.*, Journal of Chromatography B., **1026**, 36-42 (2016).
- 2) Min Liu *et al.*, BMC Complementary and Alternative Medicine., **15**, 382(2015).

This work is supported by the National Natural Science Foundation of China Key Program (no. 81530094), National Natural Science Foundation of China (No. 81403077), Natural Science Foundation of Guangdong Province (No. 2014A030310494).

## Large-scale Identification and Visualization of N-glycome with Primary Structures Using GlySeeker

(School of Chemical Science & Engineering, Tongji University, Shanghai 200092, China)

Kaijie Xiao, Yuyin Han, Zhixin Tian\*

**Key words:** N-glycome, primary structure, identification, visualization, N-glycan database search engine GlySeeker

Aberrant glycosylation has been commonly observed in various types of cancers, and quite a few glycoproteins have been approved by US Food and Drug Administration (FDA) as markers for early diagnosis; yet, effective markers with satisfactory sensitivity and specificity are still widely lacking. Mass spectrometry-based glycomics is the state-of-the-art instrumental analytical pipeline for high-throughput analysis of N-glycomes.[1-4] With the combination of CH<sub>3</sub>I permethylation, PGC enrichment, RPLC-MS/MS analysis and our recently developed N-glycan database search engine GlySeeker based on isotopic envelope fingerprinting [5, 6], large-scale identification and visualization of N-glycomes with primary structures (not only monosaccharide composition, but also sequence & linkage) have become possible. In this presentation, we will present our development of GlySeeker as well as its application in characterization of differentially expressed N-glycans in hepatocellular carcinoma HepG2 cells (vs. normal liver LO2 cells). The integrated platform can, in principle, be adopted for both qualitative and quantitative characterization of any N-glycome system.

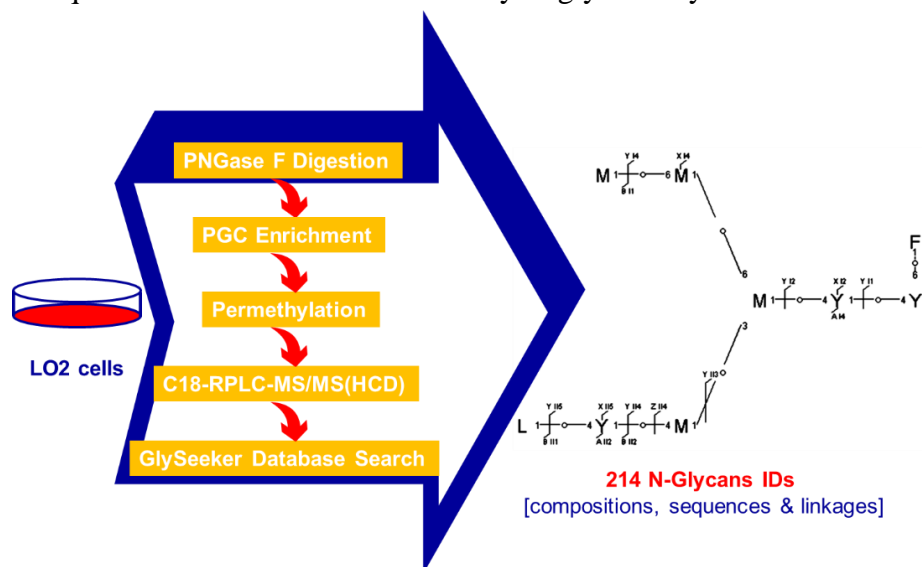


Fig. 1. Schematic diagram of N-glycome characterization using GlySeeker

### References

- [1] K. Tanabe, et al. *J Proteome Res*, **15**, 2935-2944 (2016).
- [2] L. Cheng, et al. *Oncotarget*, **7**, 61199-61214 (2016).
- [3] Y. Qin, et al. *Glycoconj J*, doi 10.1007/s10719-017-9768-5 (2017).
- [4] Y. Huang, et al. *Electrophoresis*, doi 10.1002/elps.201700025 (2017).
- [5] K. Xiao, et al. *Anal and Bioanal Chem*, doi 10.1007/s00216-018-1070-2 (2018).
- [6] K. Xiao, et al. *Rapid Commun Mass Spectrom*, **32**, 142-148 (2018).